A New High Power Factor Power Supply Using The Bang-Bang Hysteresis Current Waveshaping Control Technique

Barreto, L. H. S. C.; Pereira, A. A. (**); Farias, V. J.; Freitas, L. C. de and Vieira Jr., J. B.

Universidade Federal de Uberlândia
Centro de Ciências Exatas e Tecnologia
Departamento de Engenharia Elétrica
Campus Santa Mônica - Bloco "3N"
38400-902 - Uberlândia - MG – Brazil
Phone: 55 34 239-4166 FAX: 55 34 239-4166
Email: batista@ufu.br

(**) Universidade Federal de Goiás
Departamento de Computação
Campus Avançado de Catalão
CEP: 75.704-020 - Catalão - GO - Brazil
FAX: 55 62-441-3488

Abstract - This work presents the operation and design of a high power factor high frequency switching power supply. A good power factor is obtained using as a pre-regulator circuit an AC-DC Boost Converter associated with a non-dissipative snubber operating with high power factor and without commutation losses. The same non-dissipative snubber associated with the Forward converter, providing the soft commutation switching, is used as the DC-DC converter. A complete theoretical analysis, simulation and experimental results are presented.

1 - INTRODUCTION

The power supply unit is a very important circuit for all electronic equipments, because it provides the necessary voltages for correct work of the electronic circuits, these electronic circuits are used, usually, to perform professional or domestic equipments, for instance - computer, equipments of telecommunication, aviation and military, games, etc. These equipments are more sophisticated, then it is indispensable a power supply smaller and lighter, and more efficient. Generally, these equipments use AC as a primary power energy supply, therefore, the AC must be transformed in DC energy, because the majority of these systems require high quality DC power.

The linear power supplies are good for low power applications, but are uneconomical and inefficient when more power is required. The alternative is to use the switched mode power supplies (SMPS). This kind of power supplies presents: multi output DC voltages, constant switching frequency and reduced size and weight when compared with linear power supplies, but the input stage of the switching mode power supplies are well known to be harmonic generators. Recently, there has been great interest about the reduction of input current harmonics and power factor correction (PFC). Moreover, in many single-phase applications, mainly in power supplies, the power level can reach several kWatts; and in some situations, the input voltage can be quite high too. For these types of application the conventional Boost PFC converter has been more used due to its characteristics of dc-voltage gain, lower inductor volume and weight, and losses on the power devices, which will affect converter cost, efficiency, and power density [1], [2] and [3]. It is perfect for pre-regulator, but this converter presents commutation and conduction losses, bringing reduction in the efficiency.

Conventional Resonant and Quasi-Resonant Converters [4], [5], [6], [7] and [8] provide ZCS (Zero-Current Switching) and/or ZVS (Zero-Voltage Switching) [9], [10], and these converters can operate with high-frequency, but these techniques have load limitation, because there are current and/or voltage peaks over the switches and range of frequency control, making difficult the filter components design.

A good way to reach high frequency and high-power operation is to use the non-dissipative snubber presented in references [11], [13] and [14].

The switching mode power supply provides the transformation of one DC voltage level to another, then a DC-DC converter is used for this finality. There are several DC-DC converters that can be used in this case, but it is necessary those converters operate in high-frequency and presenting reduction of switching losses, regulated multiple output and isolation between outputs.

A DC-DC Forward converter using non-dissipative snubber that can reach high frequency and high-power operation is used in this SMPS. This converter is well suitable for this power level and it provides:

- Soft switching for full load range;
- Conduction losses are almost the same as those observed in the hard PWM converter.

2 - THE PROPOSED SMPS

The AC-DC and DC-DC non-dissipative converters are shown in Figure 1 and Figure 4 . These two converters can operate with reduced commutation losses. In these converters of the SMPS the switches S1 (Boost) and S1'(Forward) are commutated in a ZVS way and the switches S2 (Boost) and S2' (Forward) are commutated in the ZCS form due to the resonant cell, composed for resonant inductors (Lr and Lr') and resonant capacitors (Cr1, Cr2, Cr1' and Cr2'). The high power factor is obtained using the Bang-Bang Hysteresis current waveshaping control technique [12].

To simplify the analysis the converters will be studied separated, but it does not prejudice its understanding.

3 - PRINCIPLE OF OPERATION OF THE AC-DC BOOST

Figure 1 shows the Boost Converter associated with a non-dissipative snubber used like a pre-regulator.

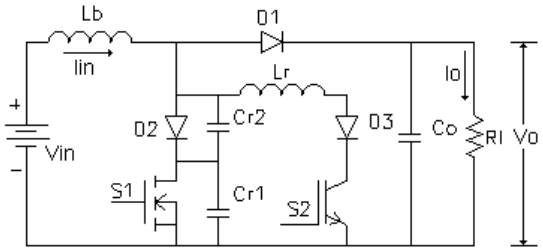

Figure 1 - Boost Converter associated with the non-dissipative snubber.

From [11] and [13], one can obtain the waveforms shown in Figure 2.

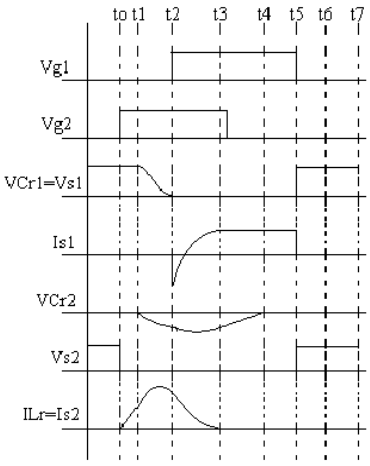

Figure 2 - Theoretical waveforms for the Boost Converter associated with a non-dissipative snubber.

From [11] and [13]. The transfer function between Vo and Vin is given by:

$$G = \frac{Vo}{Vin} = \frac{1}{1 - \left\{ D + \frac{K1}{2\pi}\left[\operatorname{Arccos}\left(-\frac{1}{X}\right) + \frac{X+1}{X\alpha} + \frac{\alpha}{2} \right] \right\}} \quad (1)$$

Where:

f_s = switching frequency;
f_0 = resonant frequency;
D = duty cycle;
X = it is the reason between Cr1 and Cr2.

$$\alpha = \frac{Iin}{Vo}\sqrt{\frac{L_R}{C_R}} \quad (2)$$

$$K1 = \frac{f_s}{f_0} \quad (3)$$

4 - CONTROL STRATEGY

The block diagram of the control circuit with the Boost power stage is shown in Figure 3. This converter operates with constant switching frequency and high power factor, using a Bang-Bang current control strategy.

The samples of the input current and line voltage are obtained from Rshu and Rt1 / Rt2 sensors. The voltage sample is rectified in the Precision Rectifier block.

The PI controller is implemented to provide the signal control (Vc) which is multiplied for the voltage reference (Vinref). Following this signal is added to the sawtooth signal generating the reference current signal (Iref). Drive signals are achieved comparing the current feedback signal, obtained in the Rshu sensor, with the reference current signal.

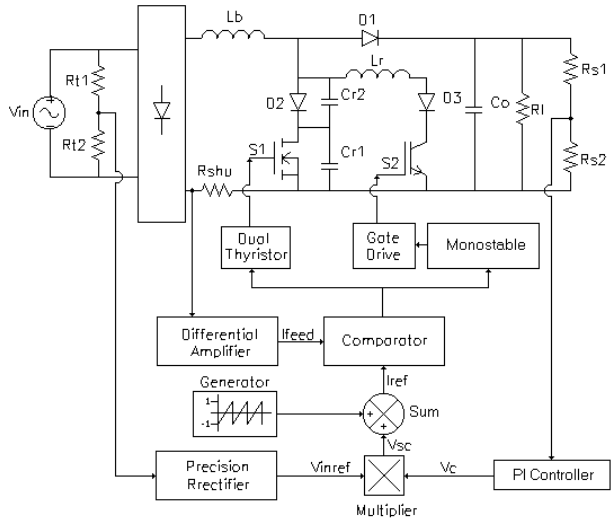

Figure 3 - Boost Converter associated with the non-dissipative snubber and the control circuit.

The signal obtained from the output comparator block is driven directly to monostable, to provide a fixed pulse, and driven to auxiliary switch S2. The same signal will drive the switch S1, when the zero voltage transition on the switch is satisfied. It is possible because switch S1 is driven in a dual thyristor mode.

5 – THE PROPOSED FORWARD CONVERTER

Figure 4 shows a simplified schematic circuit of the Forward converter associated with the non-dissipative snubber.

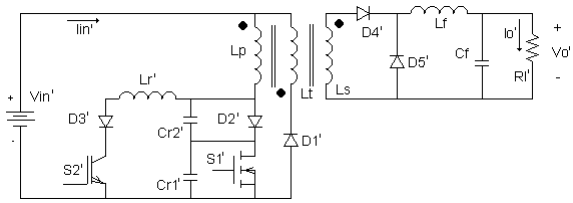

Figure 4 - Forward converter associated with the non-dissipative snubber.

Following, a theoretical analysis for the approach shown in Figure 4 is presented. The analysis begins with the description of the seven operational stages whose are divided a switching cycle of the proposed converter.

First Stage (t_1, t_2) - This stage begins when switch S2' is turned on in a ZCS way. During this stage the resonant inductor current (ILr') rises linearly from zero to the input current (Iin').

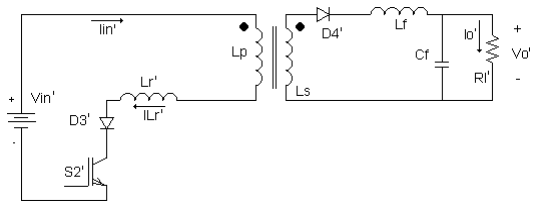

Figure 5 - First Stage (t_1, t_2).

Second Stage (t_2, t_3) - When the resonant inductor current (ILr') is equal to the input current (Iin'), this stage begins. During this stage the resonance between the resonant capacitors (Cr1' and Cr2') and the resonant inductor (Lr'), begins. In this stage the resonant capacitor 1 (Cr1') is discharged and the resonant capacitor 2 (Cr2') is charged. This stage finishes when the resonant capacitor 1 (Cr1') is completely discharged.

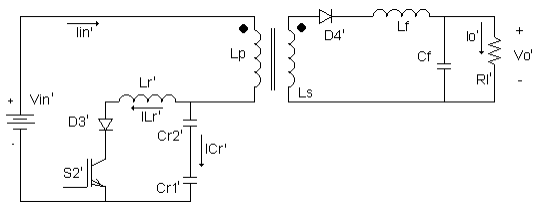

Figure 6 - Second Stage (t_2, t_3).

Third Stage (t_3, t_4) -This stage begins when the voltage on the resonant capacitor 1 (Cr1') is equal to zero. During this stage the resonant capacitor 2 (Cr2') is in resonance with the resonant inductor (Lr'), alone. When the resonant inductor current is equal to zero this stage finishes. After the resonant inductor current reaches zero the switch S2' can be turned off in a ZCS way. During this stage the main switch S1' is turned on in a ZVS way.

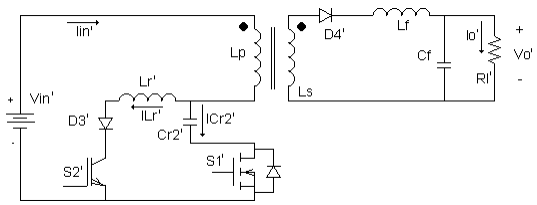

Figure 7 - Third Stage (t_3, t_4).

Fourth Stage (t_4, t_5) - This stage begins when ILr' is equal to zero, and it finishes when the voltage on resonant capacitor 2 (Cr2') is zero. During this stage the resonant capacitor 2 (Cr2') is discharged in a linear way by the input current (Iin').

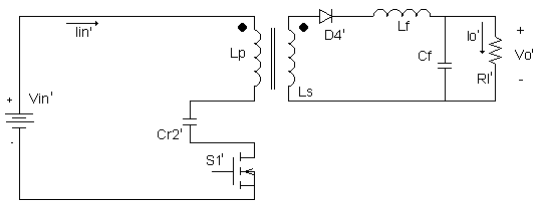

Figure 8 - Forth Stage (t_4, t_5).

Fifth Stage (t_5, t_6) - This stage begins when the voltage on the resonant capacitor 2 (Cr2') is equal to zero, turning on diode D2'. When switch S1' is turned off in a ZVS way this stage finishes. During this stage the energy is transferred from the input voltage source (Vin') to the load. This stage is responsible for the converter PWM characteristics.

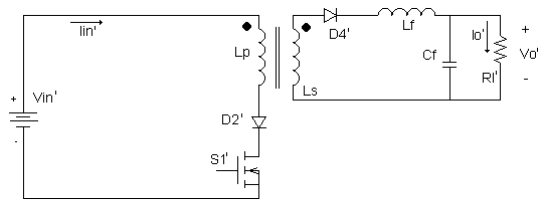

Figure 9 - Fifth Stage (t_5, t_6).

Sixth Stage (t_6, t_7) - When the main switch S1' is turned off, this stage begins. Input current flows through the resonant capacitor 1 (Cr1'), this capacitor is charged up to the output voltage (Vo'). This stage finishes when diode D1' is turned on beginning the transformer demagnetization.

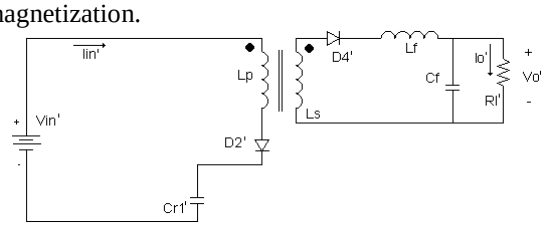

Figure 10 - Sixth Stage (t_6, t_7).

Seventh Stage (t_7, t_8) – This is the stage of the transformer demagnetization. When diode D1' is turned on, this stage begins. This stage finishes when the transformer demagnetization finishes. During this stage the transformer demagnetizes over the impute voltage source (Vin').

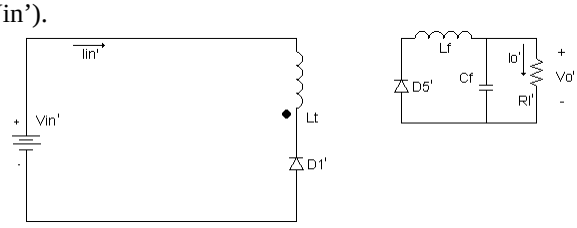

Figure 11 - Seventh Stage (t_7, t_8).

Eighth Stage (t_8, t_9) – When the transformer demagnetization finishes this stage begins. This is the freewheeling stage. This stage finishes when switch S2' is turned on, in a ZCS way, beginning the next switching cycle.

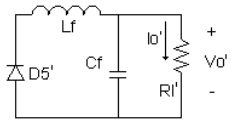

Figure 12 – Eighth Stage (t_8, t_9).

From the operating stages. The transfer function between Vo' and Vin' is given by:

$$G' = \frac{Vo'}{Vin'} = \frac{ns}{np}\left\{D' + \frac{K1'}{2\pi}\left[\operatorname{Arccos}\left(-\frac{1}{X'}\right) + \frac{X'+1}{X'\alpha'} + \frac{\alpha'}{2}\right]\right\} \qquad (4)$$

Where:

np = number of windings of the primary;
ns = number of windings of the secondary;
f_s' = switching frequency;
f_0'= resonant frequency;
D' = duty cycle;
X' = it is the reason between Cr1' and Cr2'.

$$\alpha' = \frac{Iin'}{Vin'}\sqrt{\frac{L_R'}{C_R'}} \qquad (5)$$

$$K1' = \frac{f_s'}{f_0'} \quad (6)$$

From the operating stages, one can obtain the waveforms shown in Figure 13.

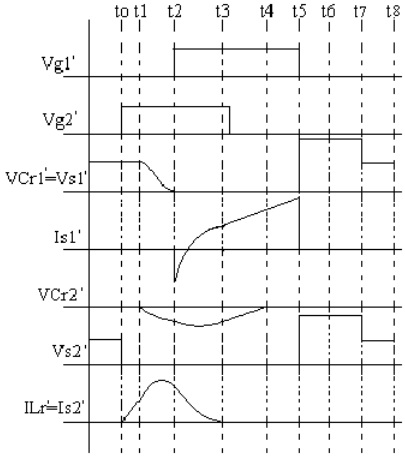

Figure 13 - Theoretical waveforms for the Forward Converter associated with a non-dissipative snubber.

In Figure 14 is shown de control strategy of Forward converter.

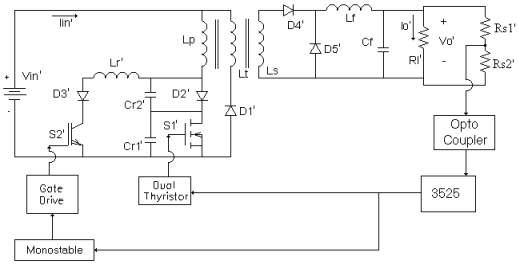

Figure 14 – Control strategy of Forward Converter.

6 – SIMULATION AND EXPERIMENTAL RESULTS

The switching mode power supply proposed was studied by simulation using the PSpice software and using the following parameter set:

S1 and S1' = IRFP460;	C_{R1} = 10nF;
S2 and S2'= Sbreak;	C_{R2} = 27nF;
D3 and D3' = Dbreak;	C_{R1}' = 7.5nF;
Other diodes = MUR1560;	C_{R2}' = 47nF;
P_0 = 600 W;	L_R and L_R' = 2.5μH;
f_S = 100kHz;	L_b = 1.5mH;
V_{in} = ~110 V;	Cf = 1mF;
C_0 = 680μF;	Vo' = 50V;
Lf = 100μH;	Io' = 12A.

A prototype of the proposed switching mode power supply was built using the following parameter set:

S1 and S1' = IRFP460;	C_{R1} = 10nF;
S2 and S2'= IRGBC20f;	C_{R2} = 27nF;
D1' = 2 x MUR1560;	C_{R1}' = 7.5nF;
Other diodes = MUR1560;	C_{R2}' = 47nF;
P_0 = 600 W;	L_R and L_R' = 2.5μH;
f_S = 100kHz;	L_b = 1.5mH;
V_{in} = ~110 V;	Cf = 1mF;
C_0 = 680μF;	Vo' = 50V;
Lf = 100μH;	Io' = 12A.

Figures 15, 16, 17, 18 and 19 show the simulation and experimental results. As can be seen the commutations of the switches occur without losses and the power factor is almost unity. Figure 15 shows the power factor correction, in the nominal load was obtained the value of 0.998.

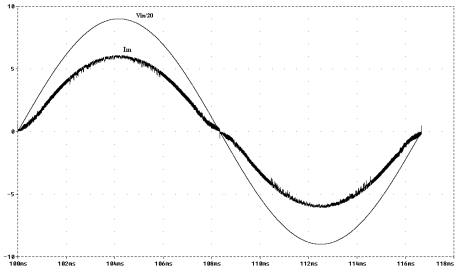

(a)

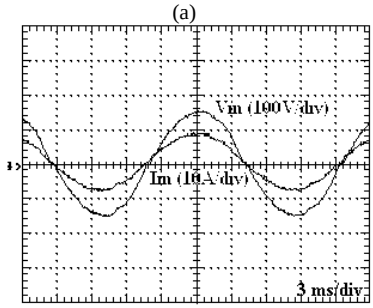

(b)

Figure 15 - Input voltage and current for nominal load:
a) simulated results;
b) experimental results.

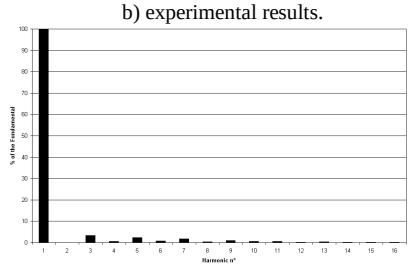

(a)

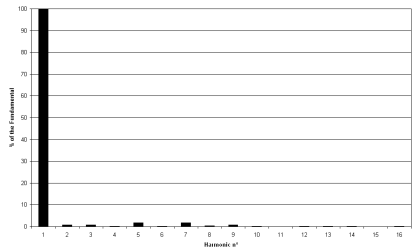

(b)

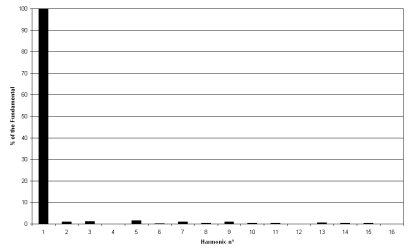

(c)

Figure 16 – Harmonic Spectrum:
(a) of the Input Current for simulated results;
(b) of the Input Voltage for experimental results;
(c) of the Input Current for experimental results.

Current and voltage THD were obtained, they are relatively low as it can be seen in figure 16. THD was calculated for the current, in the simulation and in the

experimentation, and for voltage just in the prototype. From the simulation the value of THD of current obtained was of 4.85%, for the prototype the value of current and voltage THD, were 2.84% and 2.83%, respectively.

Figure 17 shows the input of the comparator, where the pulses are generated, little interference can be seen, this is due to the used filters in the control.

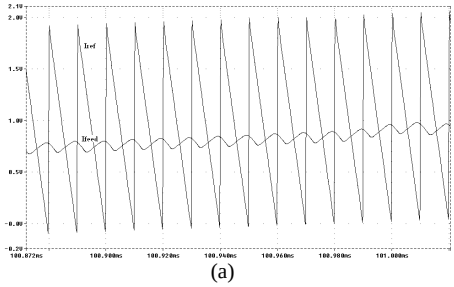

(a)

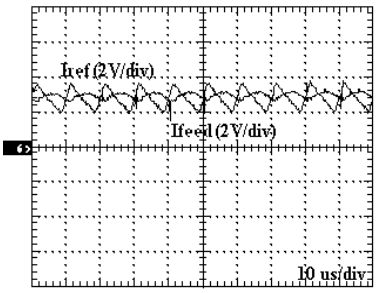

(b)

Figure 17 – Impute of the comparator:
(a) for simulated results;
(b) for experimental results.

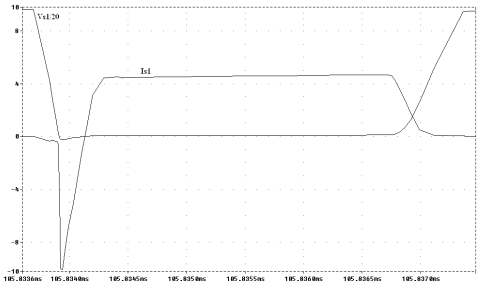

(a)

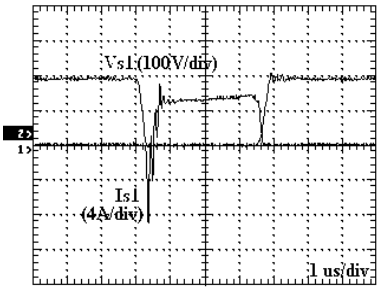

(b)

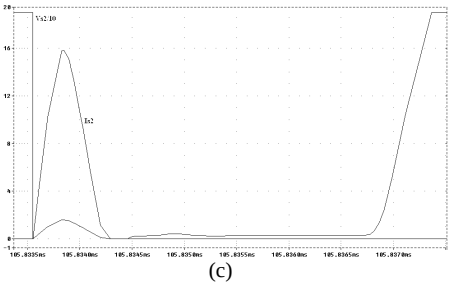

(c)

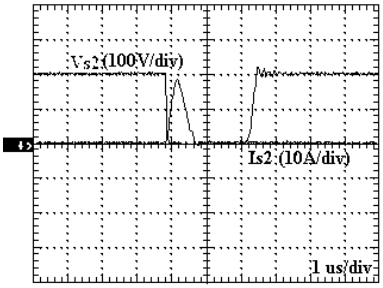

(d)

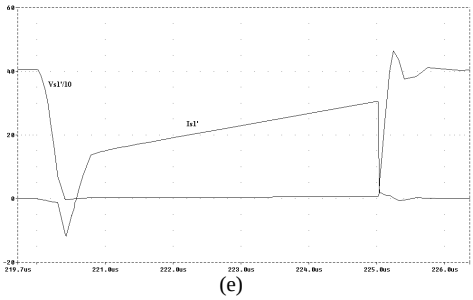

(e)

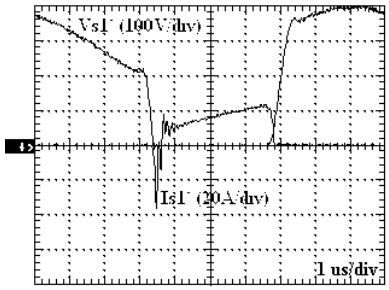

(f)

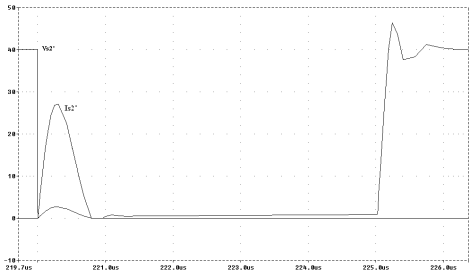

(g)

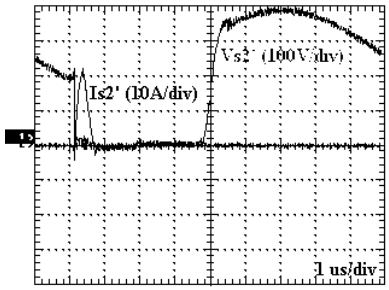

(h)

Figure 18 - Experimental Results:
a) Switch s_1 waveforms for simulated results;
b) Switch s_1 waveforms for experimental results
c) Switch s_2 (auxiliary switch) waveforms for simulated results;
d) Switch s_2 (auxiliary switch) waveforms for experimental results;
e) Switch s_1' waveforms for simulated results;
f) Switch s_1' waveforms for experimental results;
g) Switch s_2' (auxiliary switch) waveforms for simulated results;
h) Switch s_2' (auxiliary switch) waveforms for experimental results.

Figure 18 shows the commutation in the active switches, it can be seen that the main switch does not present stresses of current and/or voltage, as well as the commutations are non-dissipative. The auxiliary switch commutates with zero current.

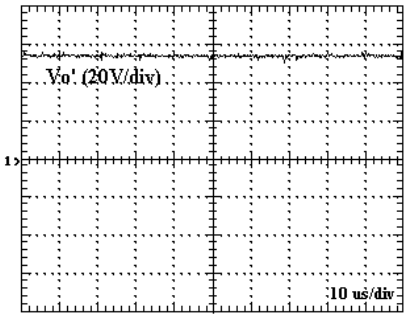

Figure 19 – Output voltage of the switch mode power supplies proposal.

Figure 19 shows the output voltage of the switching mode power supply proposed, where we can see that the source has an excellent regulation.

The graph of the Figure 20 represents the curve of the efficiency of switching mode power supply proposed, a medium efficiency of 91% is calculated.

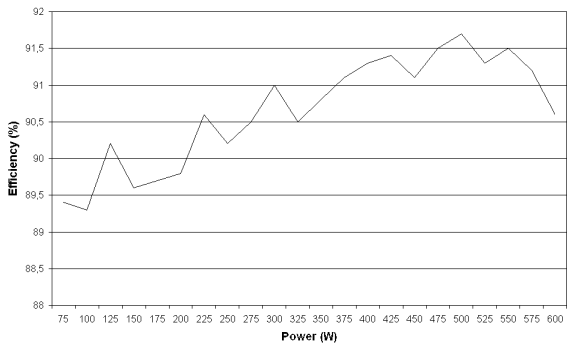

Figure 20 – Curve of efficiency.

7 – CONCLUSIONS

This paper reports the analytical, simulation and experimental developments of a SMPS using the PFC AC-DC Boost associated with a non-dissipative snubber. It has been demonstrated that the use of the Bang-Bang Hysteresis current waveshaping control technique in combination with the non-dissipative snubber permits highly efficient power factor correction pre-regulator without commutation losses. The proposed approach allows a good performance in high frequency of operation.

The SMPS presented uses a Forward converter as a DC-DC converter. This converter works with soft-commutation by using a non-dissipative snubber.

The objective initially proposed was reached, a switched source with correction of power factor (0.998), high efficiency (91%) and lower harmonic distortions (2.84% for current and 2.83% for voltage) and good regulation was analyzed theoretically, projected, simulated and implemented.

8 – REFERENCES

[1] Zhang, M.T., Jiang, Y., Lee, Fred, C.,Joavanovic, Milam M.; “Single-Phase Three-Level Boost Power Factor Correction Converter, IEEE APEC’95, PP. 434-439.

[2] - Corrêa Pinto, J. A.; Pereira, A.A.; de Freitas, L.C.; Vieira Jr.,J. B.; Farias, V.J; "A Power Factor Correction Preregulator AC-DC Interleaved Boost With Soft-Commutation", PESC'97, USA

[3] Miwa, B. A., Otten, D. M., And Schlecht, M. F., “High Efficiency Power Factor Corretion Using Interleaving Techniques”, Proceedings of APEC`92 IEEE Catalog n0 : 92CH3089-0, pp. 368-375.

[4] Lee, F. C.; “High-Frequency Quasi-Resonant Converter Technologies”, Proceedings on the IEEE, Vol. 76, no 4, April 1988.

[5] Barbi, I., Bolacell, J. C. and Vieira Jr., J. B., “A Forward Pulse-Width Modulated Quasi-Resonant Converter: Analysis, Design and Experimental Results”, IEEE IECON’89, Record, pp. 21-26, Philadelphia, Pennsylvania, USA.

[6] Barbi, I., Hey, H. L. and Vieira Jr., J. B., “A Half-Bridge Pulse-Width Modulated Zero-Current Switched Quasi-Resonant Converter”, IEEE IECON’89, Record, pp. 42-47, Philadelphia, Pennsylvania, USA.

[7] Barbi, I., Oliveira, M. A. and Vieira Jr., J. B., “A Pulse-Width Modulated Zero-Voltage-Zero-Current Switched Half-Bridge Quasi-Resonant Converter”, IEEE IECON’89, Record, pp. 54-59, Philadelphia, Pennsylvania, USA.

[8] Vieira Jr. J. B., “Quasi-Resonant Converters: New topologies, project and analysis”, PhD Thesis, UFSC, Florianópolis, SC, Brazil, 1991.

[9] Lee, F. C., Hua, G. and Leu, C. S., “Novel Zero-Voltage-Transition PWM Converters”, IEEE PESC’92, Record, pp. 55-61, Toledo, Spain.

[10] de Freitas, V. J. Farias, P. S. Caparelli, J. B. Vieira Jr., H. L. Hey, D. F. Cruz, “An Optimum ZVS-PWM DC - to - DC Converter Family: Analysis, Simulation and Experimental Results”. IEEE PESC’92, Record, pp. 229-235, Toledo, Spain, Jul. 1992.

[11] Barreto Luiz H. S. C., Pereira Adriano A., Farias Valdeir J., de Freitas Luiz C. and Vieira Jr, João B. ;”A Boost Converter Associated With A New Non-Dissipative Snubber”, IEEE APEC’98, Record pp. 1077 – 1083, Los Angeles, California, USA, Feb/1998.

[12] Tóffano R. Jr., Treviso C.H.G., Farias V.J., Vieira Jr. J.B. And de Freitas L.C.; ”A Self-Resonant-PWM Boost Converter With Unity Power Factor Operation by Using Bang-Bang Current Control Strategy With Fixed Switching Frequency”, EPE’97, Record pp. 4.454 – 4.457, Trondheim, Norway, Sep/1997.

[13] Barreto L. H. S. C., “Analysis, Project and Prototype of a Switching Power Supply, With High Power Factor, Using A New Snubber Non Dissipativo”, MSc Thesis, UFU, Uberlândia, MG, Brazil, 1999.

[14] Barreto L. H. S. C., Pereira A. A., Farias V. J., Freitas L. C. de and Vieira Jr J. B.;”A Boost Converter Associated With A New Non-Dissipative Snubber”, CBA’98, Record pp. 1155 – 1160 , Uberlândia, Minas Gerais, Brazil, Set/1998